Available online at www.sciencedirect.com
SCIENCE DIRECT
Biochemical and Biophysical Research Communications 339 (2006) 191–195
BBRC
www.elsevier.com/locate/ybbrc

Quaternary assembly and crystal structure of GDP-D-mannose 4,6 dehydratase from *Paramecium bursaria Chlorella* virus

Camillo Rosano [a], Simone Zuccotti [b], Laura Sturla [c], Floriana Fruscione [c], Michela Tonetti [c], Martino Bolognesi [d,*]

[a] *Bioinformatics and Structural Proteomics, National Institute for Cancer Research (IST), Largo R. Benzi 10, 16132 Genoa, Italy*
[b] *Department of Physics, CNR-INFM and Center of Excellence for Biomedical Research, University of Genova, Via Dodecaneso 33, 16146 Genoa, Italy*
[c] *Department of Experimental Medicine, Section of Biochemistry and Center of Excellence for Biomedical Research, University of Genova, Viale Benedetto XV 1, 16132 Genoa, Italy*
[d] *Department of Biomolecular Sciences and Biotechnology, CNR-INFM, University of Milano, Via Celoria 26, 20131 Milan, Italy*

Received 27 October 2005
Available online 10 November 2005

Abstract

GDP-D-mannose 4,6 dehydratase is the first enzyme in the de novo biosynthetic pathway of GDP-L-fucose, the activated form of L-fucose, a monosaccharide found in organisms ranging from bacteria to mammals. We determined the three-dimensional structure of GDP-D-mannose 4,6 dehydratase from the *Paramecium bursaria Chlorella* virus at 3.8 Å resolution. Unlike other viruses that use the host protein machinery to glycosylate their proteins, *P. bursaria Chlorella* virus modifies its structural proteins using many glycosyltransferases, being the first virus known to encode enzymes involved in sugar metabolism. *P. bursaria Chlorella* virus GDP-D-mannose 4,6 dehydratase belongs to the short-chain dehydrogenase/reductase protein superfamily. Accordingly, the family fold and the specific Thr, Tyr, and Lys catalytic triad are well conserved in the viral enzyme.

Keywords: *Paramecium bursaria Chlorella* virus enzyme; GDP-D-mannose dehydratase; Protein structure; Quaternary assembly; GDP-L-fucose biosynthesis

GDP-D-mannose 4,6 dehydratase (GMD) is the first enzyme in the "de novo" biosynthetic pathway of GDP-L-fucose [1]. Fucose is found in almost all organisms, from bacteria to plants and animals, where it is an essential component of glycoconjugates. Fucosylated glycans have been shown to play a fundamental role in cell-to-cell adhesion and recognition, pathogenicity, and development [2–5]. The "de novo" GDP-L-fucose biosynthetic pathway starts from GDP-D-mannose, which is initially dehydrated on the C-6 atom by GMD, leading to formation of the first intermediate compound, GDP-4-keto-6-deoxy-D-mannose [6]. The two following steps, an epimerization of the C-5 and C-3 centers, and a NADPH-dependent reduction at C-4, are catalyzed by a single enzyme, GDP-4-keto-6-deoxy-D-mannose epimerase/reductase (GMER) [7]. Both enzymes have been found in prokaryotes and eukaryotes; their amino acid sequences display good levels of evolutionary conservation [6–10].

We have recently shown that functional GMD and GMER are encoded also in the genome of *Paramecium bursaria Chlorella* virus 1 (PBCV-1) [11]. PBCV-1 is a large polyhedral DNA virus that replicates in unicellular Chlorella-like green algae and, unlike other viruses that use host-encoded enzymes in the ER-Golgi system for glycoprotein production, PBCV-1 encodes many enzymes required to glycosylate its capsid proteins [12,13]. Compared to GMD from bacterial and eukaryotic sources so far characterized, the PBCV-1 enzyme shows several

* Corresponding author. Fax: +39 02 5031 4895.
E-mail address: martino.bolognesi@unimi.it (M. Bolognesi).

0006-291X/$ - see front matter © 2005 Elsevier Inc. All rights reserved.
doi:10.1016/j.bbrc.2005.11.009

unexpected properties. In particular, PBCV-1 GMD behaves as a bifunctional enzyme, displaying the dehydratase activity but also a strong NADPH-dependent reductase activity on GDP-4-keto-6-deoxy-D-mannose (the dehydration product), leading to the formation of GDP-D-rhamnose [11]. Since both fucose and rhamnose are components of the glycans attached to the PBCV-1 major capsid protein [14], the virus-encoded enzymes could circumvent a limited supply of GDP-sugar by the algal host.

GMD, together with GMER, belongs to a branch of the short-chain dehydrogenase/reductase (SDR) homology superfamily, involved in nucleotide sugar metabolism [15]. All members have a well-conserved N-terminal region responsible for binding of the dinucleotide cofactor, hosting the family conserved Ser/Thr, Tyr, and Lys catalytic triad. GMDs from several sources have been shown to contain tightly bound $NADP^+$, which is involved in an internal redox reaction during the dehydration process [5,8]. Studies on their quaternary assemblies have indicated the presence of a functional homodimer in GMD from *Escherichia coli* [5] and in the human enzyme [8]. Conversely, recent reports on the crystal structures of GMDs from *Arabidopsis thaliana* and *Pseudomonas aeruginosa* are consistent with the enzyme assembly into homotetrameric forms [16,17].

Here we report a structural characterization of PBCV-1 GMD, in the context of our ongoing studies on the biosynthetic pathways for GDP-L-fucose production [1,6,11,18,19]. The 3.8 Å crystal structure of the viral GMD highlights conservation of the protein fold and quaternary assembly previously recognized for prokaryotic and eukaryotic GMDs, hinting at a mechanism for protein association/dissociation linked to the coenzyme redox state and active site binding.

Materials and methods

Crystallization. PBCV-1 GMD was expressed and purified as described earlier [11]. Protein solutions in the 8–10 mg/ml concentration range were used for the crystallization experiments. After searching through randomly distributed crystallization conditions, crystals of PBCV-1 GMD were reproducibly obtained by equilibrating 500 µl reservoir solution, containing 30% PEG 4000, 0.2 M sodium acetate, and 0.1 M Hepes, pH 7.5, against a droplet containing 1 µl of the reservoir solution and 1 µl of the stock protein solution. Storage of the crystallization droplets at 21 °C, for 7 days, yielded prismatic-shaped crystals of about $0.5 \times 0.07 \times 0.02$ mm^3.

Structure determination and refinement. X-ray diffraction data could be collected up to a maximum resolution of 3.8 Å, using synchrotron radiation (beamline BW7B, at DESY/EMBL, Hamburg-Germany, $\lambda = 0.8040$ Å), at 100 K. For cryoprotection the crystals were soaked in a solution containing 34% PEG 4000, 0.25 M sodium acetate, and 0.2 M Hepes, pH 7.5. Subsequent attempts to improve crystal quality, through crystallization additives, modified crystal handling, or search for a new crystal form, were consistently unsuccessful. The 3.8 Å diffraction data were integrated using MOSFLM and scaled using SCALA, from the CCP4 program suite [20]. PBCV-1 GMD crystals belong to the tetragonal space group $I4_1$ ($I4_3$), with unit cell constants: $a = b = 122.6$ Å, $c = 89.1$ Å, and $\alpha = \beta = \gamma = 90°$; a crystal packing coefficient of 2.3 Å^3/Da (44.5% solvent content) is compatible with the presence of two PBCV-1 GMD molecules (37.8 kDa each) in the asymmetric unit. The three-dimensional structure was solved by molecular replacement techniques using the program Molrep [21], using the homologous GMD from *A. thaliana* as search model ([16]; PDB code 1N7G; 47.0% sequence identity), thereby solving the space group ambiguity. Crystallographic refinement was performed using the program REFMAC5 [22], alternated with visual inspection and model re-building. This procedure allowed to build the Ile264–Arg296 segment, deleted in *A. thaliana* GMD, and to properly position one NADP(H) molecule in each active site of the PBCV-1 GMD asymmetric unit dimer. Due to the unrecoverable low resolution displayed by all PBCV-1 GMD crystals tested, a common *B*-factor value of 40 Å^2 was adopted for the whole protein molecule throughout the refinement. Data collection and refinement statistics are reported in Table 1.

Results and discussion

PBCV-1 GMD structure was solved through molecular replacement methods using as search model the structure of the homologous enzyme from *A. thaliana* [16]. The refined structure (space group $I4_1$) contains 5362 (2681×2) protein atoms and 2 NADP(H) molecules (Fig. 2); the final *R*-factor value is 0.295 (at 3.8 Å resolution, with a *R*-free value of 0.355, and close to ideal stereochemical parameters for the protein model; see Table 1). The main chain electron density map is well defined from residue Ser3 to Asn344, for both molecules present in the asymmetric unit.

As implied by the molecular replacement approach, PBCV-1 GMD tertiary structure matches closely those of homologous GMDs. A structural overlay with *A. thaliana* GMD yields a rmsd of 1.2 Å, calculated over 266 Cα pairs, the largest deviation occurring at residue Leu116 of PBCV-1 GMD (5.5 Å). Relative to *A. thaliana* GMD, the primary structure of PBCV-1 GMD is shorter by four residues at the latter site (the α4–β5 loop). Moreover, a large insertion segment (24 residues following the α8 helix, residues 261–293) gives rise to three antiparallel β-strands, a sort of compact unit, starting at residue Val265. Such a structural feature is shared by *E. coli* GMD. However, different from *E. coli* GMD, PBCV-1 GMD displays a well-defined structure in the 35–43 sequence stretch, building one rim of the nucleotide-binding domain. Such stretch, named the "RR-loop" in view of Arg residues at its boundary positions [17], does not adopt a specific secondary structure in most GMDs and is fully disordered in *E. coli* GMD [23]. The tertiary structure of PBCV-1 GMD shows very good agreement also with that of *P. aeruginosa* GMD, displaying a rmsd of 1.1 Å, calculated over 271 Cα pairs, with a maximum displacement at residue Leu116 (2.7 Å). On the other hand, *E. coli* GMD unexpectedly displays a higher rmsd value (2.5 Å, calculated over 259 Cα pairs), likely related to the absence of the bound cofactor in the three-dimensional structure available for this enzyme (see below).

Similar to other enzymes of the nucleotide-diphosphate-sugar modifying SDR superfamily (18), PBCV-1 GMD is composed of two domains: a N-terminal domain binding the NADP(H) cofactor and a smaller C-terminal domain which binds the nucleotide sugar substrate. The larger N-terminal domain adopts a modified Rossman fold structure, consisting of a seven-stranded parallel β-sheet (with 3-2-1-4-5-6-7 topological scheme) sandwiched between six

Table 1
Data collection and crystallographic refinement statistics for PBCV-1 GMD

Beamline	DESY/EMBL BW7B
λ (Å)	0.804
Resolution range (Å)	86.74–3.57
Last shell	3.59–3.57
Total reflections collected	27648
Unique reflections	7935
Redundancy	3.5
Completeness (%)	97.7
R_{merge}	0.18
$I/\sigma(I)$ (last shell)	4.9(1.9)
Resolution range used in refinement (Å)	50.00–3.80
Completeness for range (%)	98.1
Unique reflections used in refinement	6025
R free test set count	446
R factor	0.295
R free	0.355
rmsd bond lengths (Å)	0.004
rmsd angles (°)	0.575
rmsd planes (Å)	0.003

α-helices. The α2 helix, one edge of the Rossman fold domain, observed as a deformed helix in other GMD structures [16,17,23], is not present in PBCV-1 GMD due to the deletion of six residues in the region following Glu46. The C-terminal domain, by homology to other SDR enzymes, is expected to be responsible for binding of the nucleotide sugar. Its structure is less regular than the N-terminal domain, consisting of a three-helix bundle and four β-strands connected by elongated loops, protruding into the solvent. A wide cleft between the two domains hosts the NADP(H) cofactor, next to the Rossman fold topological switch point. In contrast to many dehydrogenases displaying the Gly-X-X-X-Gly-X-Gly consensus sequence close to the bound nucleotide diphosphate bridge, PBCV-1 GMD displays the Gly-X-X-Gly-X-X-Gly motif, typical of the SDR family [15,18].

The two asymmetric unit monomers of PBCV-1 GMD (see Fig. 1) are tightly associated by packing of two long α-helices (α3 and α4 helices in PBCV-1 GMD, α4 and α5 in the homologous GMDs); such an association, which builds the dimeric interface in many SDRs, gives rise to an extended intermolecular four helical bundle. In addition, two PBCV-1 GMD dimers build a tetrameric structure through crystallographic symmetry (Fig. 1). Such tetrameric assembly is based on an extended interface of parallel helices (α4 and α5), burying approximately 1265 Å^2 of protein surface, per subunit. In this tetrameric association, two adenosine moieties from symmetry-related NADP(H) molecules fall at a shortest distance of about 8.5 Å. Such a short distance between the two cofactor binding sites could indicate that dimer/tetramer quaternary structure equilibria may be affected by the presence of bound NADP(H).

Given the tight subunit packing achieved by PBCV-1 GMD, it is worth noticing that an alternate dimeric assembly, based on pairing of the 35–43 RR-loops of two symmetry related molecules, can be singled out within the tetrameric assembly described above and might be proposed as representative of an alternate dimeric species. Such an assembly is based on the swapping of the RR-loops between molecules A and A′ (B and B′), the swapped RR-loop fitting snugly into the active site cleft of facing protein molecule (Figs. 1 and 2). The surface buried, in each subunit by the interaction, is 1180 Å^2. Remarkably, inspection of the *E. coli* GMD structure indicates that in the absence of bound NADP(H) the RR-loop does not fit into the opposing subunit active site, it is disordered in the solvent, and the protein adopts the monomeric state [23]. Our results and the reported basic considerations on homologous proteins suggest that binding of the cofactor may facilitate protein aggregation through proper structuring of the active site cleft. They are also in keeping with the

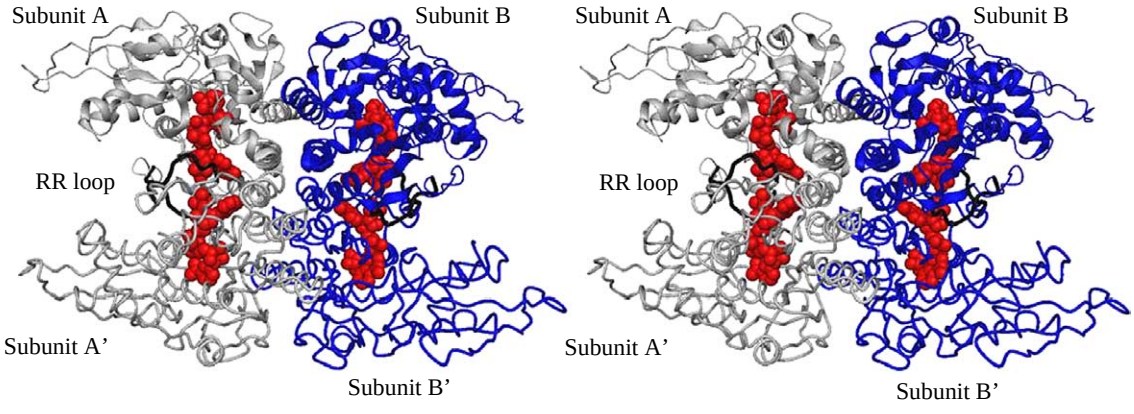

Fig. 1. Stereo view of PBCV-1 GMD quaternary structure. The protein homotetrameric species is shown, using different colors to highlight the subunit association modes described in the text. The PBCV-1 GMD asymmetric unit homodimer is shown using ribbons of the same size (blue and gray dimers, on the top and the lower half of the figure, respectively). The alternate homodimer assembly proposed (i.e., the dimeric assembly based on pairing of the 35–43 RR-loops of two symmetry related molecules) is identified by use of identical drawing colors (i.e., gray dimer on the left, blue dimer on the right, respectively). The PBCV-1 GMD bound NADP(H) molecules are shown in red. Note the swapping of RR loops (black segments) to the active site region of a facing protomer. (For interpretation of the references to color in this figure legend, the reader is referred to the web version of this paper.)

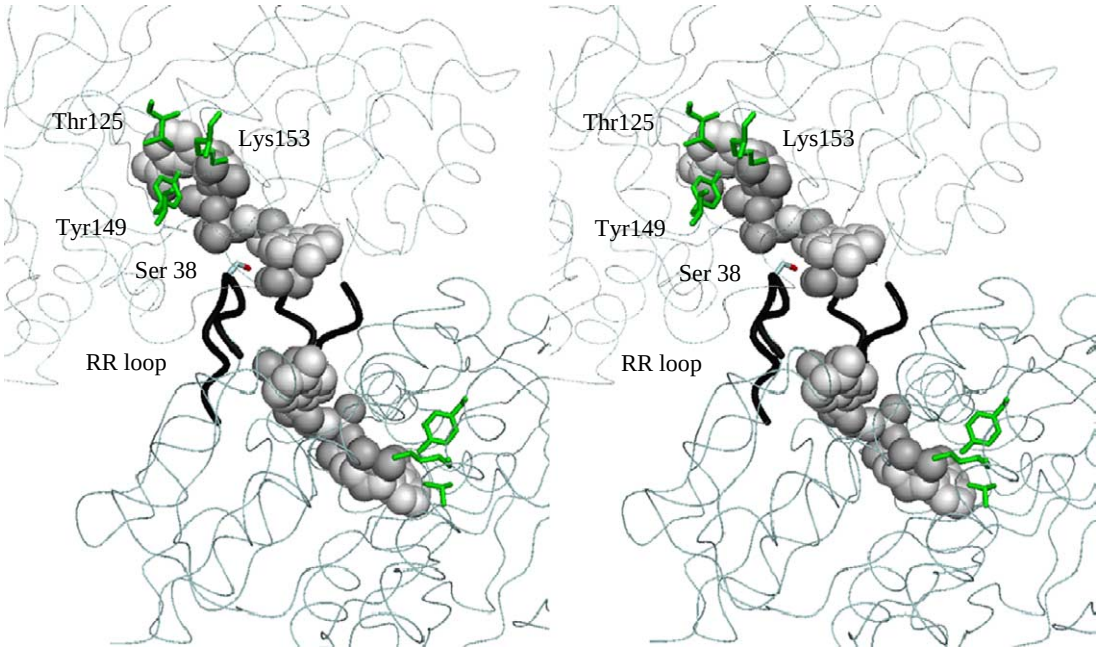

Fig. 2. Details of the intermolecular interactions between the swapped RR loop and NADP(H). The stereo figure shows the RR loop of one subunit (black), contacting NADP(H) (light gray space filling model) of the facing PBCV-1 GMD subunit. Residue Ser 38 proposed to mediate the intermolecular interaction is shown, together with the catalytic triad residues Thr125, Tyr149, and Lys153, close to the nicotinamide end of the bound nucleotide.

observed solution behavior of PBCV-1 GMD, which is found as a monomeric inactive species in the absence of NADPH, and as a dimeric active form when the reduced cofactor is present (M. Tonetti, unpublished results).

Despite the absence of any cofactor model from the molecular replacement search structure, it became clear during the crystallographic refinement that each monomer in the asymmetric unit hosts unambiguously one NADP(H) molecule in extended conformation, at the expected nucleotide binding site. The adenine moiety of the cofactor is hydrogen bonded to Asp58, being buried in a wide cavity neighboring residue Arg35. Arg35 guanidino group has been found to be stacking on the cofactor adenine in other GMD structures; in PBCV-1 GMD, however, Arg35 side chain does not display defined electron density. The adenine–ribose phosphate group is stabilized by hydrogen bonds to Thr12 and Thr37, and to Ser38′ of a neighboring molecule. Ser38′ is part of the Arg35-Arg43 RR-loop mentioned above as involved in dimer stabilization within the tetrameric assembly (Fig. 2). The RR-loop is one residue shorter in PBCV-1 GMD relative to *A. thaliana* and *P. aeruginosa* GMDs, hosting evident residue substitutions in the three proteins. Despite this, the intermolecular stabilization role through RR-loop swapping is conserved in the three enzymes (all crystallized in their holo-forms). The PBCV-1 GMD NADP(H) nucleotide diphosphate falls within hydrogen bonding distance from Ser84 and the peptidic N atoms of Gln14 and Ser84. Ala123 carbonyl O atom, residues Tyr149, and Lys153 can hydrogen bond to the nicotinamide-ribose. Notably, the nicotinamide end of NADP(H) falls close to residues Thr125, Tyr149, and Lys153 which, as described for other SDR family members, are the catalytic triad residues in PBCV-1 GMD. No electron density is however present at the expected substrate binding site, spanning the C-terminal domain.

The low resolution achieved by PBCV-1 GMD crystals allows us to draw few basic conclusions on the first viral GMD structure so far characterized. The association of SDRs in dimers, but also in tetramers, has been observed for several members of this homology superfamily, both from eukaryotic and prokaryotic sources [24]. The results presented here indicate that the same quaternary structure assembly, but also the overall protein structure and active site organization, is maintained in a viral GMD, suggesting rather complex evolutionary scenarios for the PBCV-1 genome, indeed coding for several proteins structurally homologous to both prokaryotic and eukaryotic counterparts [12]. The interplay occurring between quaternary assembly and the presence of a bound coenzyme molecule, related to the role played by swapping of the 35–43 RR loop, is a structural factor deserving renewed attention within the SDR family. In PBCV-1 GMD, the dehydratase activity is strictly dependent on the availability of NADPH, consistent with the presence of the enzyme dimeric species. Following formation of GDP-4-keto-6-deoxy-D-mannose, the oxidized coenzyme easily dissociates from GMD, leading to disorder of the RR loop, that is no longer swapped between subunits. As a result a monomeric, inactive, GMD is obtained (recovery of the full dehydratatse activity is achievable through addition of stoichiometric amounts of NADPH). Incomplete control of the coenzyme redox state, thus of the conformational states at the subunit swapped region, might have affected the PBCV-1 GMD

crystallization stage, yielding poorly ordered (low resolution diffracting) crystals. Inspection of the electron density maps obtained, however, does not highlight unexplained features, or disordered protein loops, suggesting that a significant fraction of the crystallized molecules should not display alternate conformations. It must be recalled, however, that such fraction should be of the order of at least 30% to be visible in 3.8 Å resolution electron density maps.

Acknowledgments

M.B. and S.Z. are grateful to Istituto G. Gaslini (Genova), to Fondazione Compagnia di San Paolo (Torino, Italy), and to the Center of Excellence for Biomedical Research, University of Genova, for continuous support. Support by CIMAINA, University of Milano, is acknowledged. Part of this study was supported by the Italian Ministry for University and Scientific Research FIRB Project "Biologia Strutturale" (to M.B., Contract RBLA03B3KC). C.R. is grateful to H.H. Prince Serge de Yougoslavie and to "Association Internationale Rehine Helene (AIRH) for the generous support to his research activities. M.T acknowledges the support of FIRB Project "Riconoscimento molecolare e funzionalità cellulare" and PRIN Project 2003.

References

[1] M. Tonetti, L. Sturla, A. Bisso, D. Zanardi, U. Benatti, A. De Flora, The metabolism of 6-deoxyhexoses in bacterial and animal cells, Biochimie 80 (1998) 923–931.
[2] D.J. Becker, J.B. Lowe, Fucose: biosynthesis and biological function in mammals, Glycobiology 13 (2003) 41–53.
[3] M. Maki, R. Renkonen, Biosynthesis of 6-deoxyhexose glycans in bacteria, Glycobiology 14 (2004) 1–15.
[4] R.S. Haltiwanger, J.B. Lowe, Role of glycosylation in development, Annu. Rev. Biochem. 75 (2004) 491–537.
[5] F.X. Sullivan, R. Kumar, R. Kriz, M. Stahl, G.Y. Xu, J. Rouse, X.J. Chang, A. Boodhoo, B. Potvin, D.A. Cummings, Molecular cloning of human GDP-mannose 4,6-dehydratase and reconstitution of GDP-fucose biosynthesis in vitro, J. Biol. Chem. 273 (1998) 8193–8202.
[6] M. Tonetti, L. Sturla, A. Bisso, U. Benatti, A. De Flora, Synthesis of GDP-L-fucose by the human FX protein, J. Biol. Chem. 271 (1996) 27274–27279.
[7] L. Sturla, A. Bisso, D. Zanardi, U. Benatti, A. De Flora, M. Tonetti, Expression, purification and characterization of GDP-D-mannose 4,6-dehydratase from *Escherichia coli*, FEBS Lett. 412 (1997) 126–130.
[8] A. Bisso, L. Sturla, D. Zanardi, A. De Flora, M. Tonetti, Structural and enzymatic characterization of human recombinant GDP-D-mannose-4,6-dehydratase, FEBS Lett. 456 (1999) 370–374.
[9] C.P. Bonin, I. Potter, G.F. Vanzin, W.D. Reiter, The MUR1 gene of *Arabidopsis thaliana* encodes an isoform of GDP-D-mannose-4,6-dehydratase, catalyzing the first step in the de novo synthesis of GDP-L-fucose, Proc. Natl. Acad. Sci. USA 94 (1997) 2085–2090.
[10] C.P. Bonin, W.D. Reiter, A bifunctional epimerase-reductase acts downstream of the MUR1 gene product and completes the de novo synthesis of GDP-L-fucose in Arabidopsis, Plant J. 21 (2000) 445–454.
[11] M. Tonetti, D. Zanardi, J. Gurnon, F. Fruscione, A. Armirotti, G. Damonte, L. Sturla, A. De Flora, J.L. Van Etten, *Paramecium bursaria Chlorella* virus 1 encodes two enzymes involved in the biosynthesis of GDP-L-fucose and GDP-D-rhamnose, J. Biol. Chem. 278 (2003) 21559–21565.
[12] J.L. Van Etten, Unusual life style of giant chlorella viruses, Annu. Rev. Genet. 37 (2003) 153–195.
[13] N. Nandhagopal, A.A. Simpson, J.R. Gurnon, X. Yan, T.S. Baker, M.V. Graves, J.L. Van Etten, M.G. Rossmann, The structure and evolution of the major capsid protein of a large, lipid-containing DNA virus, Proc. Natl. Acad. Sci. USA 99 (2002) 14758–14763.
[14] I.N. Wang, Y. Li, Q. Que, M. Bhattacharya, L.C. Lane, W.G. Chaney, J.L. Van Etten, Evidence for virus-encoded glycosylation specificity, Proc. Natl. Acad. Sci. USA 90 (1993) 3840–3844.
[15] H. Jörnvall, B. Persson, M. Krook, S. Atrian, R. Gonzalez-Duarte, J. Jeffery, D. Ghosh, Short-chain dehydrogenase/reductase (SDR), Biochemistry 34 (1995) 6003–6013.
[16] A.M. Mulichak, C.P. Bonin, W. Reiter, M. Garavito, Structure of the MUR1 GDP-mannose 4,6-dehydratase from *Arabidopsis thaliana*: implications for ligand binding and specificity, Biochemistry 41 (2002) 15578–15589.
[17] N.A. Webb, A.M. Mulichak, J.S. Lam, H.L. Rocchetta, R.M. Garavito, Crystal structure of a tetrameric GDP-D-mannose 4,6-dehydratase from a bacterial GDP-D-rhamnose biosynthetic pathway, Protein Sci. 13 (2004) 529–539.
[18] M. Rizzi, M. Tonetti, P. Vigevani, L. Sturla, A. Bisso, A. De Flora, D. Bordo, M. Bolognesi, GDP-4-keto-6-deoxy-D-mannose epimerase/reductase from *Escherichia coli*, a key enzyme in the biosynthesis of GDP-L-fucose, displays the structural characteristics of the RED protein homology superfamily, Structure 6 (1998) 1453–1465.
[19] S. Zuccotti, D. Zanardi, C. Rosano, L. Sturla, M. Tonetti, M. Bolognesi, Kinetic and crystallographic analyses support a sequential-ordered bi bi catalytic mechanism for *Escherichia coli* glucose-1-phosphate thymidyltransferase, J. Mol. Biol. 313 (2001) 831–843.
[20] The CCP4 Suite: Programs for Protein Crystallography. Acta Crystallogr. D 50, 1994, 760–763.
[21] A. Vagin, A. Teplyakov, An approach to multi-copy search in molecular replacement, Acta Crystallogr. D. 56 (1997) 1622–1624.
[22] G.N. Murshudov, A.A. Vagin, E.J. Dodson, Refinement of macromolecular structures by the maximum-likelihood method, Acta Crystallogr. D 53 (1997) 240–257.
[23] J.R. Somoza, S. Menon, H. Schmidt, D. Joseph-McCarthy, A.M.L. Dessen, W.S. Stahl Somers, F.X. Sullivan, Structural and kinetic analysis of *Escherichia coli* GDP-mannose 4,6 dehydratase provides insights into the enzyme's catalytic mechanism and regulation by GDP-fucose, Struct. Fold. Des. 8 (2000) 123–135.
[24] Y. Kallberg, U. Oppermann, H. Jornvall, B. Persson, Short-chain dehydrogenases/reductases (SDRs), Eur. J. Biochem. 269 (2002) 4409–4417.